Track level compensation look-up table improves antenna pointing precision

Wodek Gawronski[a], Farrokh Baher[a], Eric Gama[a]
[a]Jet Propulsion laboratory, California Institute of Technology, Pasadena, CA 91109

ABSTRACT

The pointing accuracy of the NASA Deep Space Network antennas is significantly impacted by the unevenness of the antenna azimuth track. The track unevenness causes repeatable antenna rotations, and repeatable pointing errors. The paper presents the improvement of the pointing accuracy of the antennas by implementing the track-level-compensation look-up table. The table consists of three axis rotations of the alidade as a function of the azimuth position. The paper presents the development of the table, based on the measurements of the inclinometer tilts, processing the measurement data, and determination of the three-axis alidade rotations from the tilt data. It also presents the determination of the elevation and cross-elevation errors of the antenna as a function of the alidade rotations. The pointing accuracy of the antenna with and without a table was measured using various radio beam pointing techniques. The pointing error decreased when the table was used, from 7.5 mdeg to 1.2 mdeg in elevation, and from 20.4 mdeg to 2.2 mdeg in cross-elevation.

Keywords: Microwave antennas, pointing precision

1. INTRODUCTION

The Deep Space Station (DSS) 55, shown in Figure 1, is one of the NASA Deep Space Network beam wave-guide (BWG) type antennas. The antennas are located at three Deep Space Communication Complexes: Goldstone, California, Madrid, Spain, and Canberra, Australia. At Ka-band operations, it is required to track a spacecraft with a pointing accuracy of 2 mdeg or less (rms). Repeatable pointing errors of several mdeg of magnitude have been observed during the BWG antenna calibration measurements. Systematic errors of order four and lower are eliminated with the antenna pointing model. However, repeatable pointing errors of higher order are out of reach of the model. The most prominent high-order systematic errors (of order 16 and higher) are the ones caused by the uneven azimuth track. The track is shown in Figure 2. Manufacturing and installation tolerances, as well as gaps between the segments of the track are the sources of the pointing errors that reach over 14 mdeg peak-to-peak magnitude[1], and over 20 mdeg is reported in this paper.

This paper, a continuation of our previous paper[1], presents the investigations and measurements of the pointing errors caused by the azimuth track level unevenness and shows the implementation results. Track level compensation (TLC) look-up tables were created for the DSS-25, and DSS-26 antennas (in Goldstone), DSS-34 antenna (in Canberra), and DSS-55 antenna (in Madrid). To date, the most complete and detailed results were obtained for the DSS-25 and DSS-55 antennas. In this paper, we present the DSS-55 antenna results only.

The James Clerk Maxwell Telescope[2,3] and the 34-meter Kashima antenna[4] used inclinometers to perform track profile measurements to overcome possible systematic errors. However, the results have not been published. The track level unevenness compensation is planned for the Sardinia Radio Telescope[5]. The Green Bank Telescope memo[6] reports on the pointing errors due to the azimuth track level unevenness. GBT says[7] that "in the antenna engineering and operations area work on the Green Bank Telescope azimuth track was seen as the most important." Inclinometers were used also for the thermal deformation of the IRAM telescope[8].

Optomechanical Technologies for Astronomy, edited by Eli Atad-Ettedgui, Joseph Antebi, Dietrich Lemke,
Proc. of SPIE Vol. 6273, 627316, (2006) · 0277-786X/06/$15 · doi: 10.1117/12.661259

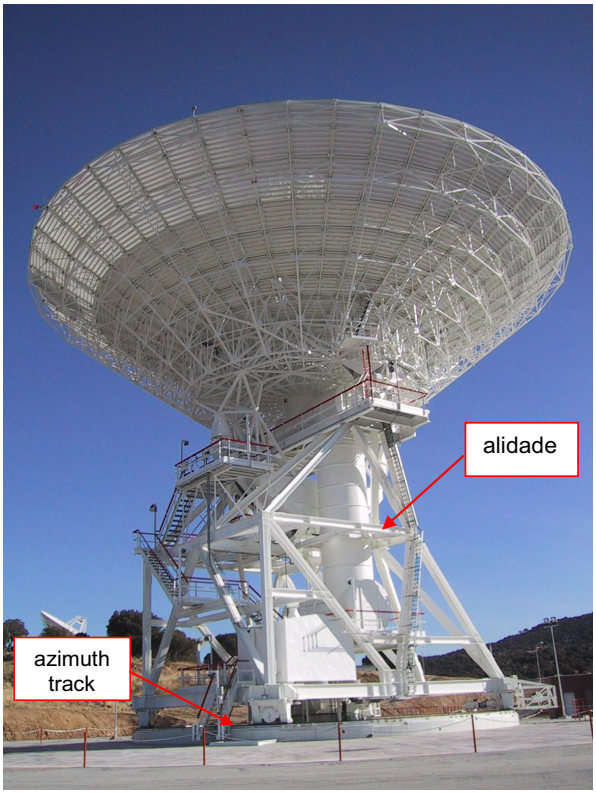

Figure 1. The DSS-55 antenna

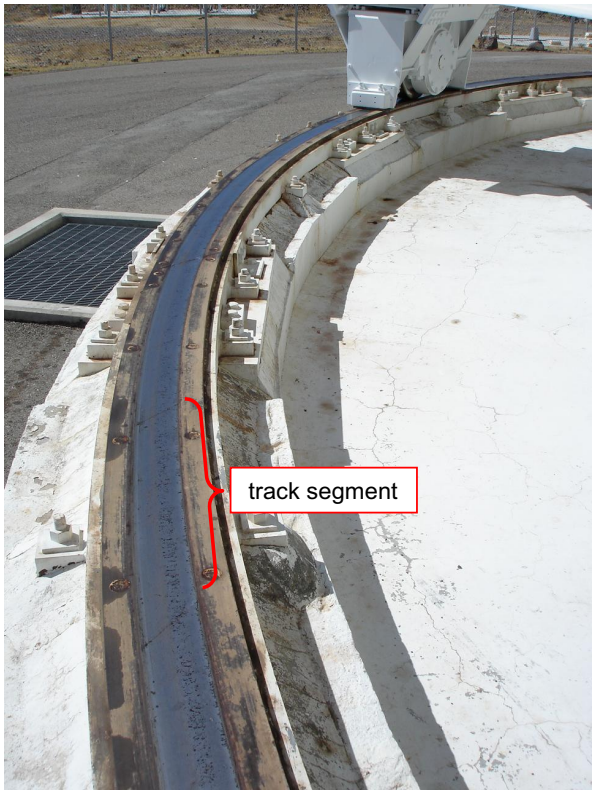

Figure 2. Azimuth track of the DSS-55 antenna

2. COLLECTION AND PROCESSING OF THE INCLINOMETER DATA

TLC system hardware consists of four inclinometers, the interface assembly, and the industrial PC computer. Four digital inclinometers (model D711 of Applied Geomechanics) are mounted on the antenna. The inclinometers are located on the alidade, as shown in Figure 3. Each inclinometer measures tilt in two axis, denoted *x* and *y*. The manufacturer describes the inclinometer rotation as tilts. Note that *x*-axis tilt is equivalent to *y*-axis rotation, and vice versa, as shown in Figure 4.

The inclinometer data were collected while the antenna moves at constant azimuth axis rate of 0.05 deg/s. Due to the environmental disturbances the inclinometer data are extremely noisy. Take for example the *x*-axis movement of the inclinometer 1 shown in Figure 5. The unfiltered data are represented by the gray line. Using a zero-phase filter to prevent filtering delay, the data is smoothed, as represented by the black line.

The additional processing included the removal of the azimuth axis tilt from the data. The tilt is present in the inclinometer data as harmonic functions in *x*- and *y*-axes, of period 360 deg, see Figure 6a,b. The best-fit algorithm applied to the DSS-55 antenna estimated the tilt magnitude 4.2 mdeg and phase 274.5 deg. The *x*- and *y*-axis movements of the inclinometer 1 after the tilt removal is shown in Figure 6a,b (red dashed line).

3. CREATING THE TLC TABLE

The TLC look-up table consists of *X*, *Y*, and *Z* rotations of the alidade, as shown in Figure 3. They are obtained from the inclinometer tilts. Namely, a rotation with respect to the antenna *x*-axis, denoted X , is a rotation with respect to the antenna elevation axis. It is measured as the *y*-tilt of the second inclinometer (a_{2y}):

$$X = a_{2y} \tag{1}$$

The *Y* rotation is a tilt of the elevation axis. It is an average of the *x*-tilts of the inclinometers 1 and 2, that is,

$$Y = 0.5(a_{1x} + a_{2x}) \tag{2}$$

The *Z* rotation of the alidade is a twist of the alidade, and is not directly measured by the inclinometers. It is determined from *x*-tilts of inclinometers 3 and 4, as follows. From Figure 7, which represents the view from the top of the alidade, we have

$$Z = \frac{d_3 - d_4}{L} \tag{3}$$

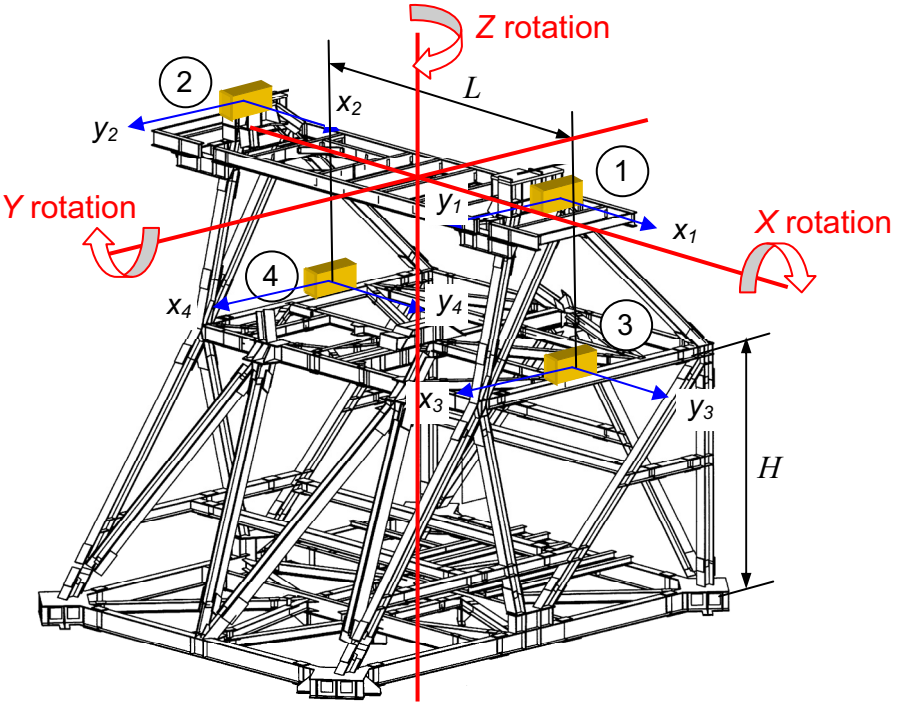

Figure 3. The location of the inclinometers at the alidade and *X*, *Y* and *Z* rotations of the alidade

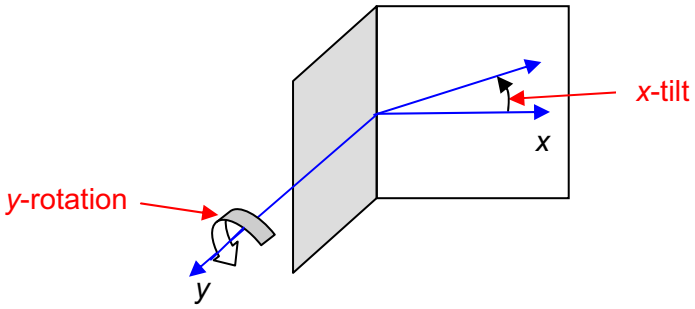

Figure 4. *x*-axis tilt is a rotation with respect to *y*-axis

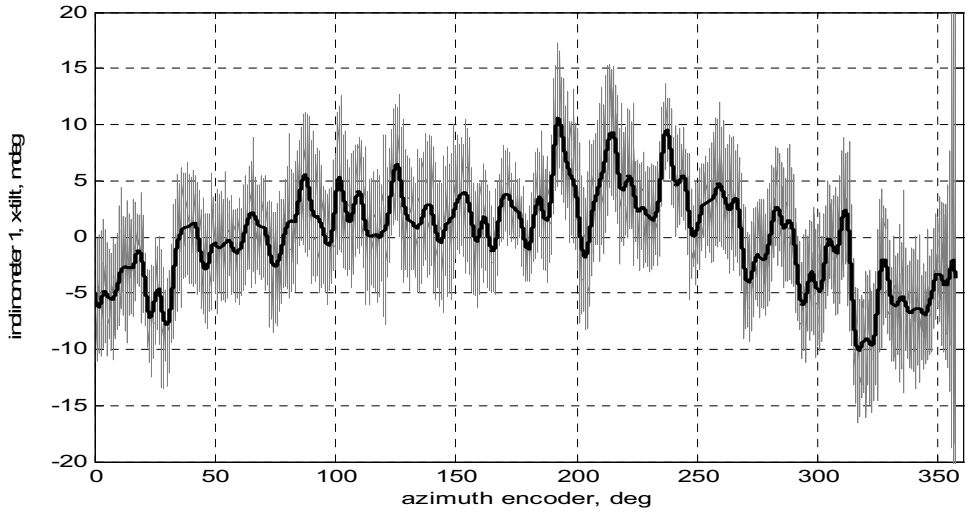

Figure 5. Raw inclinometer data (gray line) and the filtered data (black line)

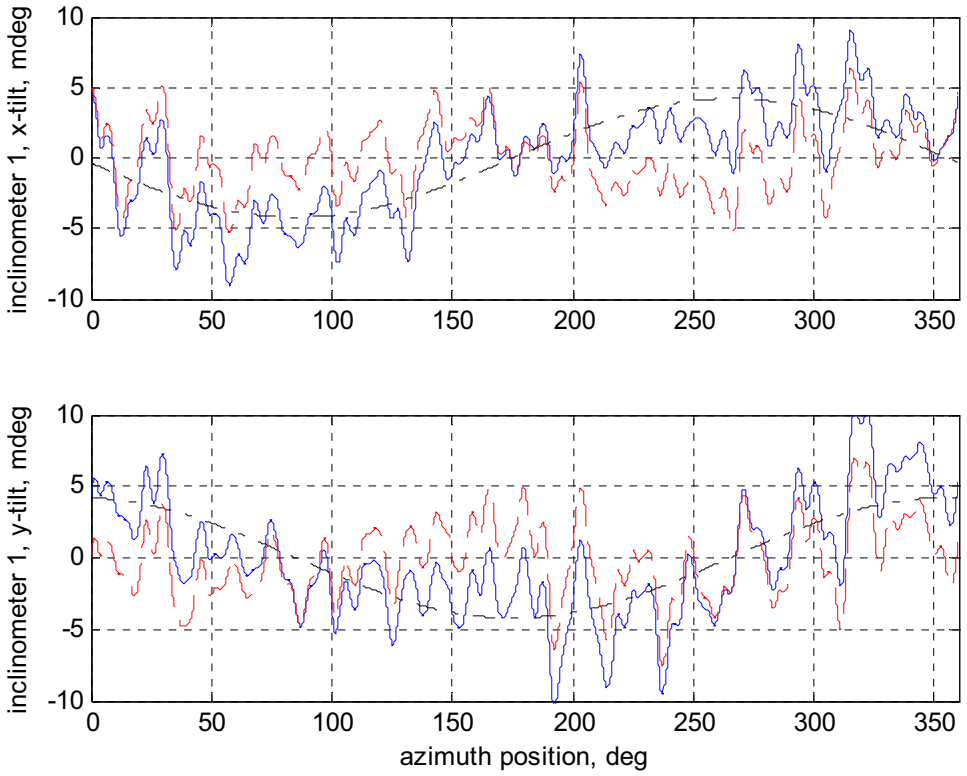

Figure 6. Removing the azimuth axis tilt from the inclinometer data (blue solid line – inclinometer data, black dash-dot line – inclinometer tilt caused by the azimuth axis tilt, and red dashed line – inclinometer data after azimuth axis tilt removal).

where d_3 and d_4 are horizontal displacements of the locations of inclinometers 3 and 4, and L=12.396 m is the distance between the two inclinometers. The displacements d_3 and d_4 are determined from the tilts of inclinometers 3 and 4, respectively, by assuming that the horizontal displacement of the alidade side due to azimuth track unevenness is caused predominantly by the rigid-body motion of each side of the alidade. This assumption was checked with the finite element model of the alidade[1], giving a 93% accuracy in estimation of displacements d_3 and d_4. It was confirmed by the

comparison of the rotations of the inclinometers located at the bottom, the middle and the top of the alidade. The rigid-body angle is measured as the *x*-tilt of the inclinometers 3 and 4 (denoted as a_{3x} and a_{4x}, respectively), therefore

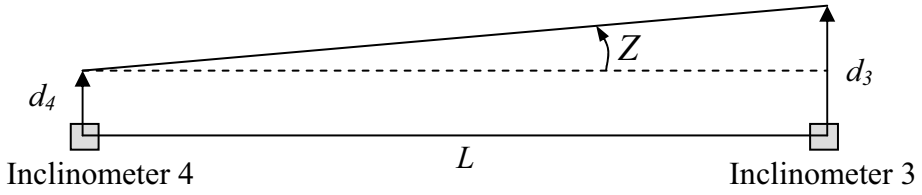

Figure 7. Top view on the inclinometers 3 and 4

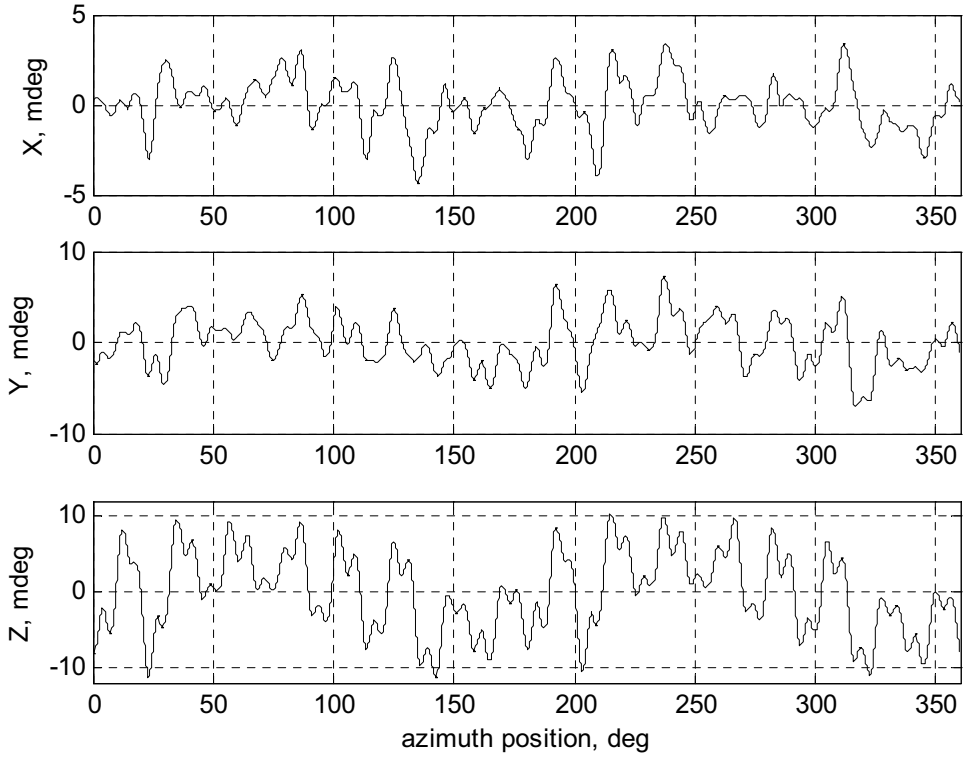

Figure 8. The TLC look-up table of the DSS-55 antenna

$$d_3 = Ha_{3x}, \qquad \text{and} \qquad d_4 = Ha_{4x} \tag{4}$$

where H is the height at which the inclinometers are located, H=9.292 m. Introducing (4) to (3) we obtain

$$Z = \frac{H}{L}(a_{3x} - a_{4x}) \tag{5}$$

where H is the alidade height, and L is the distance between the inclinometers 1 and 2. Since for the BWG antennas L=12.39 m, the ratio is $H/L = 0.75$, therefore

$$Z = 0.75(a_{3x} - a_{4x}) \tag{6}$$

The X , Y , and Z alidade rotations obtained from the inclinometer data, for azimuth angles varied from 0 to 360 deg, and for 0.1 deg azimuth angle sample size are shown in Figure 8. The plots show that the X rotation (the elevation correction) is comparatively small, and that the largest is the Z rotation. It will be shown later that the Z rotation is compensated for by the azimuth encoder and hence it is not a part of pointing error.

4. DETERMINING POINTING ERRORS FROM THE TLC TABLE

The antenna elevation error D_{EL} is simply determined as the alidade X rotation

$$D_{EL} = X \tag{7}$$

The cross-elevation error, D_{XEL} , depends on the antenna elevation position, EL , and on the alidade Y and Z rotations as illustrated in Figure 9

$$D_{XEL} = Z\cos(EL) - Y\sin(EL) \tag{8}$$

Z-rotation contributions are left out of the TLC table because this error is measurable by the azimuth encoder and therefore eliminated by the azimuth servo. The following experiment at the DSS-55 antenna was conducted to verify this hypothesis. With the antenna dish positioned at EL=30 deg. A 1 mm thick shim was placed on the azimuth track, as shown in Figure 10. The antenna was then moved slowly with constant speed in azimuth over the shim. The same antenna movement was repeated when the shim was removed. The difference between azimuth encoder reading with and without the shim is plotted in Figure 11. It shows the azimuth position rising sharply (A) when antenna is climbing the shim. But, the azimuth servo compensates for the shim disturbance (B), and the azimuth position returns to the initial position (C). As result the antenna does not need correction in z-axis, and the Z component of the TLC table shall be zero.

Based on the above experiment the following equation

$$D_{XEL} = -Y\sin(EL) \tag{9}$$

is the resulting formula for the cross-elevation error.

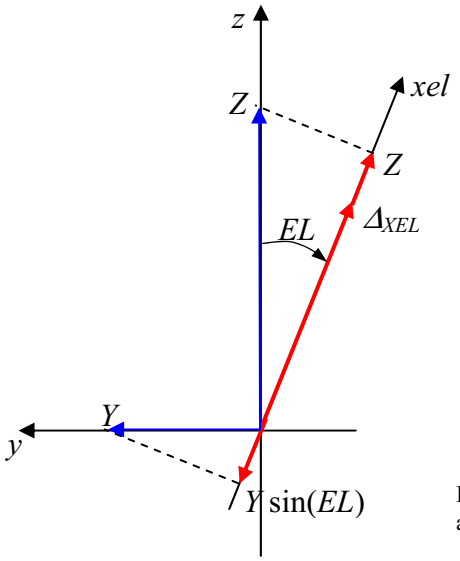

Figure 9. The relationship between the cross-elevation error and the X and Y rotations of the alidade.

Figure 10. Azimuth wheel crosses 1mm shim

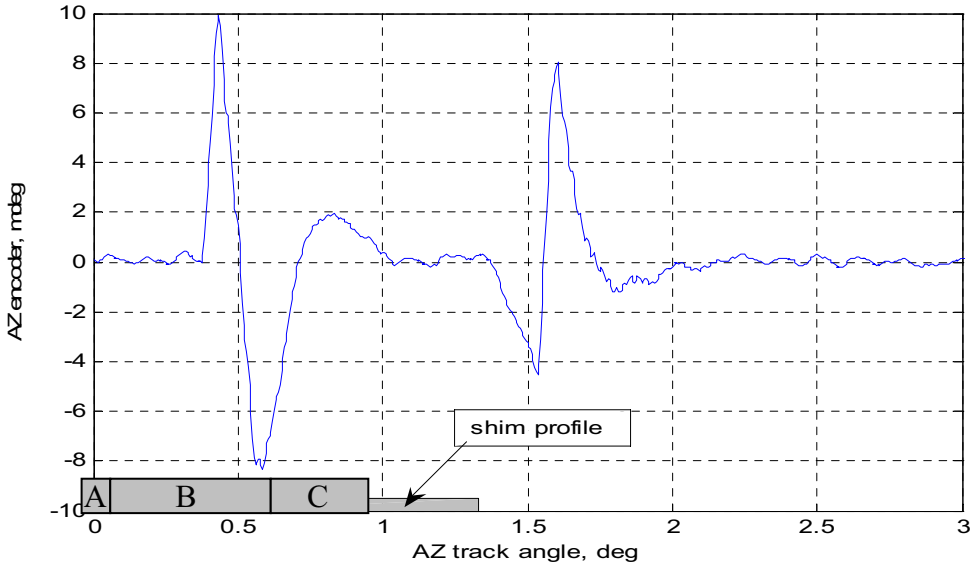

Figure 11. The azimuth encoder reading difference when crossing the shim: A) sharp rise in encoder reading at the beginning of the shim, B) azimuth servo correction to the shim disturbance, and C) stabilized azimuth position

5. ANTENNA POINTING IMPROVEMENT USING THE TLC TABLE

The improvement of pointing accuracy with the look-up table was evaluated using the radio beam pointing data. The following beam measurement techniques were used: boresight, monopulse, and conscan. The data were measured with the installed TLC table ("TLC table on") and without the TLC table ("TLC table off"). Both methods are useful in the validation of the effectiveness of the TLC table. Namely, when the table is on, the pointing errors should be significantly smaller than the errors predicted from the TLC table (or the errors obtained for the same track with the TLC table off). When the table is off, the radio beam pointing errors should match the errors predicted from the TLC table.

The measurements with the TLC table off were taken for the trajectory shown in Fig.12. Figure 13a shows that the measured elevation pointing errors and the errors predicted by the look-up table coincide. The elevation error predicted from the TLC table varies by 7 mdeg, from -3 to 4 mdeg (red line). Figure 13b shows that the cross-elevation errors (predicted and measured) coincide, when the antenna elevation position is below 72 deg, and that a deterministic residual

is uncompensated when the antenna elevation position is above 72 deg The cross-elevation error predicted from the TLC table vary by 12 mdeg, from -5 to 7 mdeg (red line); they show a "deterministic" error (for *AZ*<240 deg, where antenna elevation position above 72 deg).

The measurements of the radio beam position with TLC table on have standard deviation of 0.41 mdeg (or 1.2 mdeg peak-to-peak). while the radio beam data with the TLC table on show its standard deviation of 0.72 mdeg (or 2.2 mdeg peak-to-peak), for the antenna at elevation position below 72 deg.

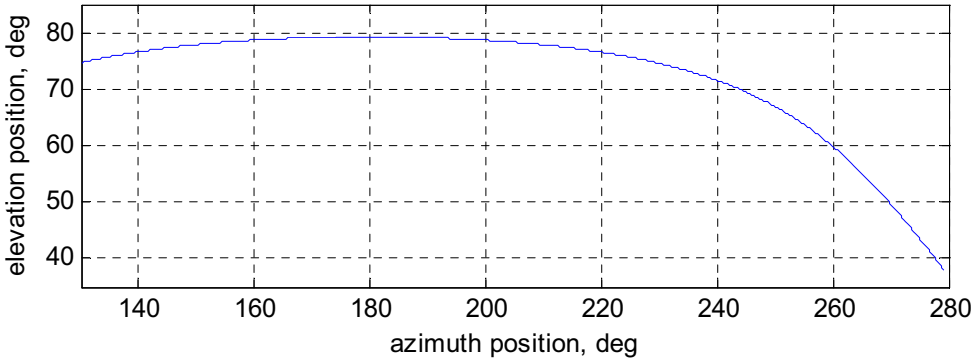

Figure 12. The DSS-55 antenna tracking trajectory.

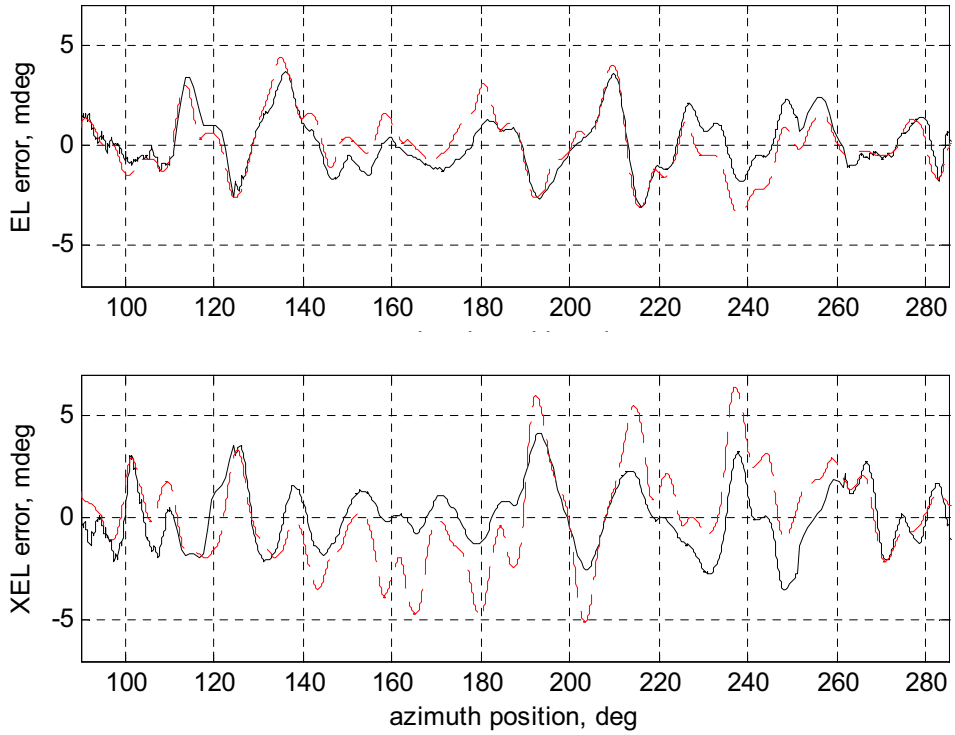

Figure 13. The DSS-55 antenna pointing errors, measured (black solid line) and predicted from the TLC table (red dashed line): (a) the elevation pointing error, and (b) the cross-elevation pointing error.

Table 1 summarizes the antenna tracking accuracy with the TLC table on and off. The elevation pointing error decreased 6 fold, and the cross-elevation pointing error decreased 10 fold.

Table 1. Peak-to-peak pointing errors of the DSS-55 antenna

	Elevation error	Cross-elevation error
Without TLC table	7.5 mdeg	20.4 mdeg
With TLC table	1.2 mdeg	2.2 mdeg

6. CONCLUSIONS

The paper presented the creation of the TLC look-up table from the inclinometer data, and the determination of the elevation and cross-elevation errors from the look-up table. It also showed that the radio beam pointing error significantly decreased from 7.5 mdeg to 1.2 mdeg in elevation, and from 20.4 mdeg to 2.2 mdeg in cross-elevation, when the look-up table is applied.

Future investigations shall determine the source of the deterministic component of the cross-elevation error when antenna elevation position is above 65 deg in order to eliminate completely the deterministic component of the pointing error.

ACKNOWLEDGMENTS

The authors would like to acknowledge the engineers from the NASA Madrid Deep Space Communication Complex: Jesús Calvo, David Muñoz, Pablo Perez, and Manuel Vázquez; and from the Jet Propulsion Laboratory: John Cucchissi, Manuel Franco, David Rochblatt, Ben Saldua, for the pointing data collection and providing technical discussions. Special thanks to Watt Veruttipong (JPL) for his technical and managerial support.

The research described in this paper was carried out at the Jet Propulsion Laboratory, California Institute of Technology, under a contract with the National Aeronautics and Space Administration.

REFERENCES

1. W. Gawronski, F. Baher, and O. Quintero, "Azimuth Track Level Compensation to Reduce Blind Pointing Errors of the Deep Space Network Antennas," *IEEE Antennas and Propagation Magazine*, 2000.
2. http://www.jach.hawaii.edu/ets/mech/mech_recent.html
3. http://www.jach.hawaii.edu/JCMT/telescope/pointing/20011006.html
4. http://www2.nict.go.jp/ka/radioastro/tdc/news_19/pdf/okubo.pdf
5. T. Pisanu, M. Morisani, C. Pernechele, F. Buffa, and G. Vargiu, "How to Improve the High Frequency Capabilities of SRT," *Proc. 7th European VLBI Network Symposium, Toledo, Spain, 2004*
6. http://wwwlocal.gb.nrao.edu/ptcs/ptcspn/ptcspn40/AzTrackSpec.pdf
7. http://www.nrao.edu/news/newsletters/nraonews94.pdf
8. A. Greve, M. Bremer, J. Penalver, P. Raffin, and D. Morris, "Improvement of the IRAM 30-m Telescope from Temperature Measurements and Finite Element Calculations," *IEEE Trans. Antennas and Propagation,* vol.53, No.2, 2005.